A subset of exoribonucleases serve as degradative enzymes for pGpG in c-di-GMP signaling

Running Title

RNases degrade pGpG to complete c-di-GMP degradation

Authors & Affiliations

Mona W. Orr[a*], Cordelia A. Weiss[a], Geoffrey B. Severin[b], Husan Turdiev[a], Soo-Kyoung Kim[a], Asan Turdiev[a], Kunquing Liu[d], Benjamin P. Tu[d], Christopher M. Waters[c], Wade C. Winkler[a], Vincent T. Lee[a#]

[a] Department of Cell Biology and Molecular Genetics, University of Maryland, College Park, MD, USA

[b] Department of Biochemistry & Molecular Biology, Michigan State University, East Lansing, MI, USA

[c] Microbiology & Molecular Genetics, Michigan State University, East Lansing, MI, USA

[d] Department of Biochemistry, University of Texas Southwestern Medical Center, Dallas, TX 75390

[*]Present address: Division of Molecular and Cellular Biology, Eunice Kennedy Shriver National Institute of Child Health and Human Development, Bethesda, MD, USA

Address correspondence to Vincent T. Lee, vtlee@umd.edu

Abstract

Cyclic-di-GMP (c-di-GMP) is a bacterial second messenger that regulates processes such as biofilm formation and virulence. During degradation, c-di-GMP is first linearized to pGpG and subsequently hydrolyzed to two GMPs by a previously unknown enzyme, which was recently identified in *Pseudomonas aeruginosa* as the 3′ to 5′ exoribonuclease Oligoribonuclease (Orn). Mutants of *orn* accumulated pGpG, which inhibited linearization of c-di-GMP. This product inhibition led to elevated c-di-GMP levels, resulting in increased aggregate and biofilm formation. Thus, the hydrolysis of pGpG is crucial to maintenance of c-di-GMP homeostasis. How species that utilize c-di-GMP signaling but lack an *orn* ortholog hydrolyze pGpG remains unknown. Because Orn is an exoribonuclease, we asked whether pGpG hydrolysis can be carried out by genes that encode protein domains found in exoribonucleases. From a screen of these genes from *Vibrio cholerae* and *Bacillus anthracis*, we found only enzymes known to cleave oligoribonucleotides (*orn* and *nrnA*), rescued the *P. aeruginosa* Δ*orn* phenotypes to wild-type. Thus, we tested addtional RNases with demonstrated activity against short oligoribonucleotides. These experiments show that only exoribonucleases previously reported to degrade short RNAs (*nrnA*, *nrnB*, *nrnC* and *orn*) can also hydrolyze pGpG. A *B. subtilis nrnA* and *nrnB* mutant had elevated c-di-GMP, suggesting that these two genes serve as the primary enzymes to degrade pGpG. These results indicate that the requirement for pGpG hydrolysis to complete c-di-GMP signaling is conserved across species. The final

steps of RNA turnover and c-di-GMP turnover appear to converge at a subset of RNases specific for short oligoribonucleotides.

Journal of Bacteriology JB Journal of Bacteriology

Importance

The bacterial cyclic-di-GMP (c-di-GMP) signaling molecule regulates complex processes such as biofilm formation. C-di-GMP is degraded in two-steps: linearization into pGpG and subsequently cleavage to two GMPs. The 3′ to 5′ exonuclease oligoribonuclease (Orn) serves as the enzyme that degrades pGpG in *Pseudomonas aeruginosa*. Many phyla contain species that utilize c-di-GMP signaling but lack an Orn homolog and the protein that functions to degrade pGpG remains uncharacterized. Here, systematic screening of genes encoding proteins containing domains found in exoribonucleases revealed a subset of genes encoded within the genomes of *Bacillus anthracis* and *Vibrio cholerae* that degrade pGpG to GMP and are functionally analogous to Orn. Feedback inhibition by pGpG is a conserved process as strains lacking these genes accumulate c-di-GMP.

Introduction

Bis-(3′-5′)-cyclic dimeric guanosine monophosphate (c-di-GMP) was originally described in 1987 by the Benziman lab as an allosteric activator of cellulose synthase in *Acetobacter xylinum* (since renamed *Komagataeibacter xylinus*) (1). C-di-GMP is utilized by many bacterial species to govern behaviors such as biofilm formation, motility, virulence, development, and cell cycle progression, making c-di-GMP a crucial regulator of bacterial lifestyle transitions. In general, high levels of c-di-GMP promote a sessile, biofilm forming lifestyle while low levels of c-di-GMP promote a motile, planktonic lifestyle (see (2) for a comprehensive review of c-di-GMP signaling).

In their initial report, the Benziman lab demonstrated that c-di-GMP is synthesized from two GTP molecules by enzymes with diguanylate cyclase (DGC) activity. C-di-GMP is degraded to two GMP molecules via a two-step process. First, it is hydrolyzed into linear 5'-phosphoguanylyl-(3',5')-guanosine (pGpG) by enzymes the authors referred to as phosphodiesterase A. This linearization process can be inhibited by Ca^{2+} ions (1) while the subsequent hydrolysis of pGpG to two GMPs is not inhibited by Ca^{2+}, which the authors interpreted as evidence for a second, distinct enzyme which they termed phosphodiesterase B (1). Numerous follow-up experimental and bioinformatics studies revealed the motifs and domains for DGC activity (GGDEF domains) (3-5) and c-di-GMP linearization activity (EAL (4, 6, 7) and HD-GYP (8) domains), yet the identity of the enzyme responsible for pGpG cleavage remained unknown. While EAL domain and HD-GYP proteins have been shown to degrade

pGpG in vitro, their contribution to pGpG turnover in bacterial cells remains under investigation. Recently, two publications identified Orn as the primary PDE-B in *Pseudomonas aeruginosa* (9, 10). Using cell lysates, we showed that ^{32}P-labeled pGpG is turned over at a much lower rate in the PA14 Δ*orn* compared to wild type (9). The Δ*orn* strain likely continued to express EAL and HD-GYP domain proteins, but their contribution towards pGpG turnover was less than 5% of Orn, indicating that Orn is the primary enzyme responsible for pGpG hydrolysis in vivo.

While c-di-GMP signaling is used across the bacterial domain, homologs of *orn* are restricted to Betaproteobacteria, Deltaproteobacteria Gammaproteobacteria, and Actinobacteria (9). For bacterial phyla that utilize c-di-GMP signaling but lack *orn* homologs, these organisms must encode another group of enzymes that fulfill the role of Orn in pGpG cleavage. Orn is a 3´ to 5´ exoribonuclease that is the major enzyme responsible for degrading short oligoribonucleotides in *Escherichia coli*. Orn was first isolated from *E. coli* in the 1970's and shown to degrade short polyA oligos (5-mer and shorter) in vitro (11, 12). The *orn* gene is essential in *E. coli*. To determine the function of Orn in vivo, a temperature-dependent mutant was generated by introducing a chromosomal interruption in the *orn* locus while supplying *orn* on a temperature-sensitive plasmid (13). Upon growth of this temperature-dependent *orn* mutant *E. coli* at the non-permissive conditions, the strain accumulated oligoribonucleotides that are 2-5 nucleotides long (13). In bacterial species that do not encode an *orn* homolog, other RNases were later identified to degrade oligoribonucleotides by

109 screening for genes that rescue growth of the *E. coli orn* mutant. Genes that
110 rescued the *orn* mutant included NrnA and NrnB, which are widely found in
111 Firmicutes (14, 15), and NrnC, which is widely found in Alphaproteobacteria (16).
112 However, direct evidence of a role in degradation of short RNA in vivo was
113 lacking. In addition, two RNases, YhaM and RNase J1, from *B. subtilis* also
114 partially rescued the *E. coli* conditional *orn* deletion mutant (15). In vitro, the 3´ to
115 5´ exoribonuclease YhaM (17) can degrade 5-mer oligo RNA, but was able to
116 degrade oligo DNA at a faster rate, suggesting that DNA could be a preferred
117 substrate (15). The 5´ to 3´ exoribonuclease RNase J1 (18) had low activity in
118 vitro against 5-mer cytosine and adenine (15). These reports suggest that other
119 RNases may degrade pGpG to terminate c-di-GMP signaling in species that lack
120 *orn*. Currently these candidates have not been experimentally tested for
121 hydrolysis of pGpG and their effects on c-di-GMP signaling. We thus used a
122 similar complementation approach to assay the effect of RNases on pGpG
123 turnover.

124 *P. aeruginosa* Δ*orn* mutants are viable, but have increased levels of
125 cytosolic c-di-GMP due to pGpG feedback inhibition, resulting in elevated c-di-
126 GMP-regulated processes such as biofilm formation (19, 20). We hypothesized
127 that genes encoding domains found in known RNA exonucleases could cleave
128 pGpG in species that do not encode *orn* and should be able to restore the
129 behavior of the *P. aeruginosa* Δ*orn* strain to wild type. Thus, we identified genes
130 that contained domains found in RNA exoribonucleases from *B. anthracis*, an
131 organism that lacks *orn,* and *V. cholerae*, another species that encodes *orn* and

is well-known to utilize c-di-GMP signaling and thus may encode additional proteins for pGpG turnover. These genes were tested for their ability to degrade pGpG through complementation of the *P. aeruginosa* Δ*orn* strain. Of the genes tested, only the known "nanoRNases" NrnA, NrnB, and NrnC could reduce aggregation of the *P. aeruginosa* Δ*orn* strain to wild type levels. Cells that express NrnA, NrnB and NrnC reduced levels of pGpG and c-di-GMP found in the *P. aeruginosa* Δ*orn* strain. Purified recombinant NrnA, NrnB and NrnC proteins were able to cleave pGpG in a manner similar to Orn. *Bacillus subtilis* lacking both *nrnA* and *nrnB* accumulated c-di-GMP. These results demonstrate that a specific subset of RNases act to hydrolyze pGpG, indicating that RNases serve as the final processing enzyme to terminate c-di-GMP signaling across bacteria.

Results

A screen identifies exoribonucleases that rescue cell aggregation and biofilm formation in *P. aeruginosa* PA14 Δ*orn*

A bioinformatic approach was used to identify candidate exoribonucleases for screening to identify additional enzymes responsible for turning over pGpG. Previously reported exoribonucleases in *E. coli* and *B. subtilis* include Oligoribonuclease, RNase B, RNase BN, RNase D, RNase J, RNase PH, RNase R, RNase T, PNPase, YhaM and Nrn proteins (21-24). These proteins were used as a starting point for bioinformatic identification of putative exoribonucleases based on Pfam domains (see Table S1). The Pfam HMM model obtained from

155 the Pfam database version 31 (March 2017) was searched against the complete
156 proteomes of *B. anthracis* str. Ames and *V. cholerae* serotype O1 using the
157 Hmmer 3.1b2 hmmsearch command (25), and resulted in a list of fifty-one unique
158 protein sequences with a signficant E-value as reported by Hmmer (See Table
159 S1) (26). Of these fifty-one, fifty genes (*polC* (*BA3955*) was not available) were
160 obtained from the *B. anthracis* and *V. cholerae* (27) Gateway clone set libraries
161 and introduced into a replicative plasmid in *P. aeruginosa*.

162 The PA14 Δ*orn* strain has elevated levels of pGpG and c-di-GMP resulting
163 in increased autoaggregation (Fig. 1) (9). The ability of each of the 50 genes to
164 cleave pGpG was tested by trans complementation of the PA14 Δ*orn* to reduce
165 autoaggregation. Expression of the PA14 *orn* (orn_{Pa}) complemented the PA14
166 Δ*orn* mutant and prevented aggregate formation, whereas the vector control
167 aggregated. Expression of genes encoding RNase B, RNase BN, RNase D,
168 RNase J, RNase PH or PNPase domains in Δ*orn* did not prevent aggregation
169 indicating that they do not hydrolyze pGpG (Fig. 1). Of the genes encoding the
170 RNase T domain, only *VC0341* (orn_{Vc}) from *V. cholerae* was able to reverse
171 aggregation (Fig. 1). For genes encoding DHH or DHHA1 domains, only *BA4852*
172 *(*$nrnA_{Ba}$*)* from *B. anthracis* prevented aggregation.

173 In addition to aggregation, the Δ*orn* strain forms more pellicle biofilm (9).
174 The pellicle biofilm was assayed using a crystal violet microtiter plate biofilm
175 assay (28). Complementation of a PA14 Δ*orn* mutant with orn_{Pa} decreased
176 biofilm two-fold compared to the empty vector ($p < 0.05$, Fig. 2A). Expression of
177 *BA4852* ($nrnA_{Ba}$) and *VC0341* (orn_{Vc}) reduced the biofilm similar to expression of

178 *orn*$_{Pa}$ ($p > 0.05$) while expression of other RNases tested had no effect in the
179 Δ*orn* strain (Fig. 2A). Similar to the aggregation assay, only *VC0341* (*orn*$_{Vc}$) and
180 *BA4852* (*nrnA*$_{Ba}$) were able to reduce the enhanced biofilm formation of PA14
181 Δ*orn*. These results suggest that Orn and NrnA are able to degrade pGpG in *V.*
182 *cholerae* and *B. anthracis*, respectively.
183 Both *BA4852* (*nrnA*$_{Ba}$) and *VC0341* (*orn*$_{Vc}$) are 3′ to 5′ exoribonucleases
184 with known activity against short oligoribonucleotides. NrnA from *B. subtilis* was
185 originally idientified from a screen that rescued the growth of an *E. coli orn*
186 conditional mutant (14). From similar screens, other RNases from *Bacillus*
187 *subtilis* and *Caulobacter crescentus*, namely *nrnB*, *rnjA*, *yhaM* and *nrnC*, were
188 also identified that could hydrolyze short oligoribonucletides in vitro (14-16). We
189 therefore asked whether these proteins could cleave pGpG by assaying for
190 complementation of the PA14 Δ*orn* strain. *nrnA*, *nrnB*, *rnjA*, and *yhaM* were
191 cloned from *B. subtilis* 168 and *nrnC* was cloned from *C. crescentus* CB15 and
192 expressed in PA14 Δ*orn*. Expression of *B. subtilis nrnA* (*nrnA*$_{Bs}$), *B. subtilis nrnB*
193 (*nrnB*$_{Bs}$), and *C. crescentus nrnC* (*nrnC*$_{Cc}$) were able to prevent aggregation of
194 the PA14 *orn* mutant while *yhaM* and *rnjA* were not (Fig. 2B). These strains were
195 also assayed for pellicle biofilm formation. Complementation with *nrnA*$_{Bs}$, *nrnB*$_{Bs}$
196 and *nrnC*$_{Cc}$ reduced A_{595} readings to 0.15 ± 0.02, 0.14 ± 0.2, and 0.15 ± 0.02,
197 respectively, as compared to the vector control A_{595} readings 0.47 ± 0.05 (Fig.
198 2C). This reduction is similar to complementation with PA14 *orn*. Expression of *B.*
199 *subtilis rnaseJ1* (*rnjA*$_{Bs}$)and *B. subtilis yhaM* (*yhaM*$_{Bs}$) did not prevent
200 aggregation, but resulted in a modest reduction in biofilm with A_{595} readings of

201 0.31 ± 0.02 and at 0.36 ± 0.04, respecively (Fig. 2C). When combined with the
202 aggregation data, expression of *rnjA*$_{Bs}$ and *yhaM*$_{Bs}$ do not efficiently complement
203 the Δ*orn* mutant. Since pGpG accumulation causes decreased c-di-GMP
204 turnover via feedback inhibition of the phosphodiesterase responsible for
205 linearizing c-di-GMP, these data suggest that the genes *nrnA*, *nrnB*, and *nrnC*
206 could degrade pGpG in species that do not have *orn*.
207
208 Orn, NrnA, NrnB and NrnC convert pGpG to GMP
209 The elevated c-di-GMP-related phenotypes seen in the PA14 Δ*orn* mutant
210 strain was shown to be complemented by *orn*$_{Pa}$, but not catalytically inactive
211 alleles of *orn*$_{Pa}$ (9, 10). As previously reported (9), the rate of pGpG turnover in
212 whole cell lystates was barely detectable after 20 mins incubation in the empty
213 vector control, while plasmid-provided PA14 *orn* showed full conversion of pGpG
214 to GMP by 20 mins, with a half life of ~6 mins (Fig. 3A). To determine the ability
215 of each of the RNases to degrade pGpG, the lysates of PA14 Δ*orn* expressing
216 each RNase from *B. anthracis* and *V. cholerae* were tested for their ability to
217 hydrolyze ^{32}P-pGpG to ^{32}P-GMP. Of the strains expressing RNases from *B.*
218 *anthracis*, only *BA4852* (*nrnA*$_{Ba}$) decreased the pGpG half life to 0.23 minutes
219 (Fig. 3B). Of the strains expressing RNases from *V. cholerae*, *VC0341* (*orn*$_{Vc}$)
220 reduced the pGpG half life to 0.25 minutes (Fig. 3C), while the expression of
221 other RNases did not alter rates of pGpG degradation. When complemented with
222 *nrnA*$_{Bs}$, *nrnB*$_{Bs}$, and *nrnC*$_{Cc}$, the pGpG half life was decreased to 16.5 minutes 2.7
223 minutes and 1.5 minutes, respectively (Fig. 3D). Complementation with the other

RNases had similar pGpG hydrolysis rates to the empty vector control. These results suggest that these genes act on pGpG turnover in a manner similar to *orn* in *P. aeguinosa*.

To support the enzymatic activity of NrnA, NrnB and NrnC against pGpG, purified recombinant $NrnA_{Bs}$, $NrnB_{Bs}$, and $NrnC_{Cc}$ proteins were tested for the ability degrade pGpG. As expected, all were able to convert pGpG to GMP. When using 10 nM of each enzyme, the pGpG turnover rates were determined to be 517.4 ± 7.846 nM/min for Orn_{Vc}, 338.1 ± 14.3 nM/min for $NrnA_{Bs}$, 271 ± 26.31 nM/min for $NrnB_{Bs}$ and 150.6 ± 14.49 nM/min for $NrnC_{Cc}$ (Fig. 4).

HD-GYPs do not cleave pGpG in cells lacking *orn*

Previous studies have shown that HD-GYPs can cleave both c-di-GMP and pGpG in vitro (8). This has led to the suggestion that proteins containing the HD-GYP domain can act to both linearize c-di-GMP and cleave pGpG in vivo. However, deconvolution of the in vivo pGpG hydrolysis activity of HD-GYP from Orn was difficult due to essentiality of *orn* in other proteobacterial species. Using the viable *P. aeruginosa* Δ*orn* strain, we asked whether HD-GYP proteins can cleave pGpG by expressing each of the nine genes from *V. cholerae* that contain a HD-GYP domain in an Δ*orn* background. Lysates from these strains were tested for pGpG turnover by addition of ^{32}P-pGpG. Similar to the vector control, expression of any of the HD-GYP genes failed to increase pGpG hydrolysis (Figure 5). Since expression of Orn_{Vc} was able to restore pGpG hydrolysis, these results indicate that HD-GYP proteins do not cleave pGpG in vivo.

247 The intracellular concentration of pGpG and c-di-GMP in *P. aeruginosa* PA14
248 Δ*orn* is reduced by complementation with *nrnA*, *nrnB*, *nrnC*, *VC0341*, and
249 *BA4852*

250 To confirm that these changes in phenotype were due to reducing c-di-
251 GMP in the complementation strains, nucleotides were extracted from wild type
252 PA14 and the PA14 Δ*orn* strains containing empty vector or vector expressing
253 wild type orn_{Pa}, $nrnA_{Bs}$, $nrnB_{Bs}$, $nrnC_{Cc}$, *VC0341* (orn_{Vc}), and *BA4852* ($nrnA_{Ba}$)
254 and the levels of c-di-GMP and pGpG were detected by LC-MS/MS. The PA14
255 strain with vector control had 2.2 ± 0.4 μM pGpG, while PA14 Δ*orn* strain with
256 vector control had 17.4 ± 3.7 μM pGpG. Complementation of the PA14 Δ*orn*
257 strain with all genes tested reduced pGpG and c-di-GMP levels (Table 1).
258 Together, these results demonstrate that a specific subset of RNases can cleave
259 pGpG to terminate c-di-GMP signaling.
260
261 *B. subtilis* 168 Δ*nrnA* Δ*nrnB* double mutant and Δ*nrnA* Δ*nrnB* Δ*yhaM* triple mutant
262 have elevated levels of c-di-GMP

263 The ability of $nrnA_{Bs}$ and $nrnB_{Bs}$ from *B. subtilis* to complement *P.*
264 *aeruginosa* Δ*orn* suggests that these enzymes could be responsible for pGpG
265 cleavage in *B. subtilis* in a manner that is analogous to Orn function in *P.*
266 *aeruginosa*. Thus, we generated an unmarked Δ*nrnA* Δ*nrnB* double mutant in *B.*
267 *subtilis* and assayed for c-di-GMP levels using a fluorescent riboswitch reporter
268 of c-di-GMP levels. This riboswitch reporter construct consists of a constitutively
269 active promoter followed by a c-di-GMP-specific riboswitch from *B. licheniformis*

found upstream of the *lch* operon (*lchAA* UTR) fused to *yfp*. When the riboswitch is bound to c-di-GMP, it forms a terminator prior to *yfp*, resulting in lower fluorescence levels; when the riboswitch is not bound to c-di-GMP, it folds differently permitting transcription elongation through the *yfp* gene, resulting in elevated fluorescence (Fig. 6A). As a control, we used a constitutively active promoter without the riboswitch before the *yfp* reporter (P_{const}-*yfp*, Fig. 6A). As expected, the control reporter showed no differences in fluorescence between the wild type and the Δ*nrnA* Δ*nrnB* double mutant, with the same histogram distribution of fluorescence intensity in both strains (Fig. 6B, 6D). Inserting the *lchAA* UTR containing the c-di-GMP-specific riboswitch between the promoter and *yfp* is expected to render *yfp* expression sensitive to c-di-GMP levels. The Δ*nrnA* Δ*nrnB* had very low fluorescence compared to wild type indicating that c-di-GMP is indeed higher in this strain (Fig. 6C, 6E). As previously reported in *P. aeruginosa* (9, 10), this could be due to pGpG accumulation that competitively inhibits linearization of c-di-GMP. Although YhaM could not rescue aggregation in our assay in *P. aeruginosa*, (Fig. 2B) it could partially reduce pellicle biofilm formation (Fig. 2C). These data, in conjunction with the report that expression of *yhaM* could partially rescue an *E. coli orn* mutant and purified YhaM could turn over RNAs (15), led us to also generate an unmarked Δ*yhaM* mutant. The Δ*yhaM* had similar YFP levels as the parental 168 strain (Fig. S1). Furthermore, the Δ*nrnA* Δ*nrnB* Δ*yhaM* triple mutant had similar results (Fig. S2) as the Δ*nrnA* Δ*nrnB* double mutant. These results indicate that NrnA and NrnB are the enzymes primarily responsible for degradation of pGpG in *B. subtilis*.

To support the changes in c-di-GMP observed with the fluorescent riboswitch reporter construct, c-di-GMP and pGpG extracted from wild type *B. subtilis* and the Δ*nrnA* Δ*nrnB* strains were quantified by LC-MS/MS in which pGpG and c-di-GMP generated two daughter ions (Table 2). For the wild type, the concentration of pGpG was below the limit of detection. In contrast, the Δ*nrnA* Δ*nrnB* double mutant strain exhibited 1.9 µM of pGpG. For c-di-GMP, wild-type bacteria had 1 µM while the Δ*nrnA* Δ*nrnB* double mutant strain had 3. This 3-fold increase agrees with the effect on the fluorescent c-di-GMP reporter. These results demonstrate that NrnA and NrnB degrade pGpG in *B. subtilis* and suggest that product inhibition of c-di-GMP linearization by pGpG is a widespread phenomenon.

Discussion

A subset of RNases degrade pGpG

Only Orn, NrnA, NrnB and NrnC can degrade pGpG. These four genes have previously been referred to as “nanoRNases” to describe the enzymes that can cleave “extremely short oligonucleotides” that are shorter than microRNA (14). pGpG and other linearized dinucleotides from signaling cyclic dinucleotides are two-nucleotide-long RNA molecules and represent appropriate substrates for nanoRNases. Despite being functionally similar, these four proteins contain different domains and different catalytic sites. Orn belongs to the RNase T superfamily (PFAM PF00929), NrnA and NrnB belong to the NrnA family with two adjacent DHH and DHHA1 domains (PF01368 and PF02272) (14, 15) and NrnC belongs to the RNase D superfamily (PF01612) (16). Nonetheless, these specific proteins appear to be distinct from other members of their family since other RNases and proteins that share these domains do not appear to cleave pGpG.

Whether additional proteins that were not identified in this study can turn over pGpG remains an outstanding question. It is possible that the transgenic approach used in this screen could result in false negatives and yet-unidentified exoribonuclease families would not have been included in the candidate for screening. A more general question is what are the total number and identity of exoribonucleases in prokaryotes. The most well characterized exoribonucleases are in two model organisms: *E. coli* and *B. subtilis*. *E. coli* encodes Orn, PNPase, Rbn RNase II, Rnd, Rnr, Rph and Rnt (21). Of the RNases found in *E. coli*, *B. subtilis* encodes only PNPase, Rph and Rnr (22). In the past decade, a number

of additional exoribonucleases have been characterized in *B. subtilis* including RNase J, NrnA, NrnB and YhaM (14, 15). Thus, there likely are additional yet uncharacterized genes that degrade short oligonucleotides and thus can cleave pGpG and other linear dinucleotide intermediates of c-di-nucleotide turnover. The enzymes that complement PA14 Δ*orn* were previously identified through their ability to rescue lethality in a conditional *orn* mutant in *E. coli*. However, while YhaM and RNase J also rescued growth of the *E. coli orn* mutant, they did not complement the biofilm phenotypes observed in PA14 Δ*orn*. These differences indicate that complementation of Orn essentiality in *E. coli* is a distinct phenotype from complementation of the *orn* activity in *P. aeruginosa*. Future experiments using the PA14 Δ*orn* strain as a surrogate host can allow identification of genes encoding enzymes from targeted organisms or from complex microbiomes.

Enzymes that cleave linear dinucleotides are required to reduce cellular concentration of cyclic dinucleotides.

The termination of cyclic di-nucleotide signaling requires cleavage of the linear dinucleotide intermediate. In the absence of Orn in *P. aeruginosa*, pGpG is not degraded and can competitively inhibit linearization of c-di-GMP (9, 10) (Figure 7). As a consequence, c-di-GMP accumulates, leading to prolonged signaling and enhanced c-di-GMP dependent phenotypes (9, 10). Data shown here for *B. subtilis* indicate that NrnA and NrnB degrade pGpG in this organism. YhaM is not likely to be important in pGpG turnover since the c-di-GMP

riboswitch reporter showed similar c-di-GMP levels in the parental 168 strain and the Δ*yhaM* single mutant. As observed in *P. aeruginosa*, the loss of the primary enzymes responsible for pGpG hydrolysis in *B. subtilis* leads to accumulation of pGpG and c-di-GMP. These results suggest that feedback inhibition by pGpG on the enzymes that linearize c-di-GMP is a conserved property of c-di-GMP signaling. This feedback inhibition appears to also hold true for c-di-AMP signaling. C-di-AMP is linearized by enzymes that contain HD (29) and DHH-DHHA1 domain (30). Recent studies of PDE2 in *Staphylococcus aureus* revealed that this protein cleaves pApA in c-di-AMP signaling (31). Furthermore, in the absence of *pde2*, *S. aureus* cells accumulate both pApA and c-di-AMP (31) (Figure 7). Together, these studies suggest that feedback inhibition by the linear dinucleotide product of cyclic di-nucleotide turnover may be conserved. For cGAMP (32), linearization to pApG is mediated by three V-cGAP enzymes (33). How the pApG linear product of cGAMP is hydrolyzed to mononucleotide is currently unknown. Since cGAMP is produced in *V. cholerae*, we anticipate that Orn_{Vc} can serve to degrade both pApG and pGpG dinucleotides. Future studies in additional organisms will reveal whether feedback inhibition of linearization enzyme by linear dinucleotides is a general property of the known bacterial cyclic dinucleotide signaling molecules: c-di-GMP, c-di-AMP and cGAMP (Figure 7).

Proteins containing HD-GYP domain may not cleave pGpG in cells

Previous studies of HD-GYP proteins demonstrated that these proteins are able to degrade c-di-GMP and pGpG in vitro (2). In vivo studies in *V. cholerae*

373 revealed that expression of HD-GYP proteins reduced c-di-GMP levels (34).
374 Furthermore, lysates of *E. coli* overexpressing of *V. cholerae* HD-GYP domain
375 proteins was able to both degrade c-di-GMP into pGpG and subsequently to
376 GMPs (35). However, the cleavage of pGpG to GMP cannot be specifically
377 attributed to HD-GYP proteins due to the presence of Orn in the *E. coli* strain
378 background. To clearly test pGpG hydrolysis activity of proteins containing a HD-
379 GYP domain without Orn, we tested lysates of *P. aeruginosa* Δ*orn* expressing
380 each of the HD-GYP genes from *V. cholerae*. Since expression of these genes
381 failed to increase pGpG cleavage, these results provide additional evidence that
382 HD-GYP do not function as the main pGpG degrading enzymes in vivo (9, 10).
383
384 NanoRNases degrade pGpG.
385 Unlike the linearization step of c-di-GMP, which relies on c-di-GMP-
386 specific phosphodiesterases, our results suggest that the degradation of pGpG
387 does not appear to require a pGpG-specific enzyme. Instead, the turnover of
388 pGpG appears to be carried out by a subset of RNases. These RNases, dubbed
389 “nanoRNases”, were identified in screens to find genes able to rescue growth in
390 an *E. coli* conditional *orn* mutant and were shown to be able to turn over short
391 oligoribonucleotides in vitro (14-16). However, although RNase J1 and YhaM
392 were shown to partially rescue the *E. coli orn* growth defect (15), we did not
393 observe that these enzymes were able to hydrolyze pGpG or rescue the *P.*
394 *aeruginosa orn* biofilm and aggregation phenotypes, suggesting that not all
395 enzymes possessing nanoRNase activity have pGpG degrading activity.

Nevertheless, the final steps of c-di-GMP and RNA turnover appear to intersect at RNases. Thus, the relative affinity for and rate of cleavage of oligoribonucleotides of different sequence and length may matter during periods in which bacteria need to rapidly remove c-di-GMP. Whether this overlap in source of oligoribonucleotides substrates for these RNases has consequences for cellular regulation or mRNA turnover is at present an open question.

The current experiments have focused on the identification of the enzymes responsible for cleaving pGpG. Since nanoRNases are hypothesized to cleave all short oligoribonucleotides regardless of sequence, we also expect them to have activity against the linearized form of the other two cyclic dinucleotide signaling molecules (pApA from c-di-AMP and pApG from cAG). Whether the linear cAG can also engage in product inhibition is currently unknown. However, the finding that all cyclic di-nucleotides share the final processing enzymes that are also responsible for degrading 2-mer RNAs would not be surprising.

412 **Materials and Methods**

413 *Strains and culture conditions*

414 The strains, plasmids, and primers used in this study are listed in Tables
415 S2, S3, and S4, respectively. Bacteria were grown in LB or LB-agar
416 supplemented with 50 µg/mL carbenicillin at 37 °C except when otherwise noted.
417 Plasmids were induced with 1 mM IPTG. All *B. subtilis* strains in this study are
418 derived from 168. To make Δ*yhaM,* Δ*nrnA* Δ*nrnB,* and Δ*nrnA* Δ*nrnB* Δ*yhaM*,
419 strains harboring gene knockouts of locus tags BSU29250, BSU18200 and
420 BSU09930 were obtained from the BKE collection. The erythromycin-resistance
421 cassette inserted in each locus was then removed in each strain, and markerless
422 deletions were created through transformation with pDR244 ((36), Bacillus
423 Genetic Stock Center). A series of transformation protocols were performed with
424 each BKE strain as well as pDR244 until the double and triple mutant strains
425 were achieved. Removal of the erythromycin-resistance cassette was verified by
426 Sanger sequencing. For construction of the fluorescent *yfp* reporters used in this
427 study, integration at the *amyE* locus of 168 was performed with plasmids derived
428 from pJG019 (GenBank: KX499653.1). To construct pRSL_F4, the *lchAA* leader
429 sequence (complete sequence is provided in the supplemental materials) was
430 synthesized (GenScript) and inserted at the HindIII restriction site of the vector.
431 pJG019 and pRSL_F4 were transformed into 168, Δ*yhaM,* Δ*nrnA* Δ*nrnB*, and
432 Δ*nrnA* Δ*nrnB* Δ*yhaM* by using cells induced for competence through growth in
433 nitrogen limiting media (37).
434

Cloning

The *V. cholerae O1 biovar El Tor str. N16961* and *B. anthracis* Gateway compatible ORFeome libraries were obtained from BEI Resources. The ORFs were moved into the desired expression vectors (see Table S2 for primers) using LR-clonase enzyme II (Invitrogen) and introduced into chemically competent *E. coli* strain T7Iq (NEB) following the manufacturer's protocols. The *B. subtilis nrnA*, *nrnB*, *rnjA* and *yhaM* and the *C. crescentus nrnC* were cloned using the primers shown in Table S1.

Protein purification

His_{10}-VC0341, His_{10}- BA4852, His_{10}-NrnA, His_{10}-NrnB, His_{10}-NrnC, and His_{10}-YhaM were purified from *E. coli* T7Iq strains containing expression plasmids (Table S2) as described previously (38). Briefly, strains were grown in LB with appropriate antibiotic at 37°C overnight, subcultured in fresh media and grown to OD_{600} ~ 1.0 when protein production was induced with the addition of 1 mM IPTG. Induced bacteria were pelleted and resuspended in 10 mM Tris, pH 8, 100 mM NaCl, and 25 mM imidazole and frozen at -80°C until purification. Proteins were purified over a Ni-NTA column followed by desalting on a Sephadex G-25 column into reaction buffer. Proteins were flash frozen in liquid nitrogen for storage at -80°C until use.

Synthesis of radiolabeled dinucleotides

457 ^{32}P-pGpG was generated by the linearization of ^{32}P-c-di-GMP with RocR
458 from *P. aeruginosa*. For this reaction, ^{32}P-c-di-GMP (0.167 µM final) was
459 incubated with RocR (20 µM final) in 10 mM Tris, pH 8, 100 mM NaCl and 5 mM
460 $MgCl_2$ at room temperature for 1 h and the reaction was stopped by heat
461 inactivation at 98 °C for 10 min, then passed over a 3 kDa molecular weight
462 cutoff column to remove the protein. ^{32}P-c-di-GMP was enzymatically
463 synthesized as previously described (39). Purity was checked by TLC.
464
465 *Cell lysate and enzymatic activity assays*
466 The activity of whole cell lysates and purified proteins against ^{32}P-pGpG
467 was assayed as previously described (9). Briefly, 0.1 µM of purified in reaction
468 buffer (50 mM Tris, pH 8, 100 mM NaCl, and 5 mM $MgCl_2$ for NrnA, NrnB, NrnC,
469 and YhaM; 50 mM Tris, pH 8, 100 mM NaCl, and 5 mM $MnCl_2$ for Orn) was
470 incubated with 0.1 mM of pGpG spiked with 4 pM ^{32}P-pGpG tracer. For cell
471 lysates, PA14 Δ*orn* carrying the indicated complementation vectors were grown
472 overnight, subcultured 1:100 into fresh LB supplemented with carbenicillin, and
473 induced with 100 mM IPTG and grown at 37°C or 30°C as indicated to OD_{600} ~
474 0.4 with shaking. The cultures were pelleted and resuspended in 1/10th volume of
475 reaction buffer, adjusted to the same OD_{600}, and supplemented with 10 µg/mL
476 DNase, 250 µg/mL lysozyme, 10 mM PMSF, and lysed by sonication. At
477 indicated times, aliquots were removed and the reaction stopped by adding an
478 equal volume of 0.2 M EDTA, pH 8, and heated at 98 °C for 10 min.
479

480 *Thin-layer chromatography*

481 Performed as previously described (9). Briefly, 0.5 µL of each sample was
482 spotted on polyethyleneimine-cellulose TLC plates (EMD Chemicals), dried, and
483 developed in mobile phase consisting of 1:1.5 (vol:vol) saturated NH_4SO_4 and 1.5
484 M KH_2PO_4, pH 3.60. The TLC plate was dried and imaged using Fujifilm FLA-
485 7000 phosphorimager (GE) and the intensity of the radiolabel was quantified
486 using Fujifilm Multi Gauge software v3.0.

487

488 *Microtiter plate crystal violet biofilm assay*

489 Briefly, overnight cultures were diluted 1:100 in LB and grown as static
490 cultures in a 96-well polystyrene plate (Greiner) at 30 °C inside a humidified
491 chamber for 24 h. The cultures were washed of planktonic cells and stained with
492 crystal violet as previously described (28). The A_{595} was measured on a
493 SpectraMax M5 spectrophotometer (Molecular Devices).

494

495 *Aggregation assay*

496 Cultures of *P. aeruginosa* strains were grown in 10 mL LB with appropriate
497 antibiotic and IPTG induction for 24 h at 37 °C with shaking. Culture tubes were
498 allowed to settling at room temperature for 30 mins and photographed.

499

500 *Fluorescence microscopy & quantification*

501 *B. subtilis* 168 WT, Δ*nrnA* Δ*nrnB*, and Δ*nrnA* Δ*nrnB* Δ*yhaM*-derived
502 reporter strains were grown at 37˚C on LB plates supplemented with 1.5% Bacto

503 agar and 5 ug/mL chloramphenicol, when appropriate. Single colonies were used
504 to inoculate liquid MSgg medium (40) and grown at 37˚C shaking overnight. The
505 following day, cultures of each strain were inoculated 1:50 on fresh medium and
506 grown at 37˚C shaking until reaching an optical density at 600 nm (OD_{600}) of 1.0.
507 Aliquots of these cultures were placed on 1.5% low-melting agarose MSgg pads
508 and allowed to dry for 10 minutes. Agarose pads were inverted onto a glass
509 bottom dish (Willco Wells). Cells were imaged at room temperature using a Zeiss
510 Axio-Observer Z1 inverted fluorescence microscope, equipped with a Rolera EM-
511 C_2 electron-multiplying charge-coupled (EMCC) camera, and an environmental
512 chamber. Fluorescence intensity per cell was quantified using Oufti analysis
513 software (41). Images were analyzed and adjusted with FIJI software (42).
514
515 *Quantification of Intracellular c-di-GMP and pGpG in P. aeruginosa*
516 Extraction, quantification and CFU determination were performed as
517 previously described (9) using previously published MS and UPLC parameters
518 (43, 44). Briefly, *P. aeruginosa* strains were grown overnight in LB at 37 °C with
519 shaking, subcultured 1:100 in LB, and grown at 37 °C with shaking. Cells were
520 pelleted, resuspended in 100 µL ice-cold 40:40:20 (vol:vol:vol) MeOH,
521 acetonitrile, and water with 0.1 N formic acid, incubated 30 min at −20 °C for
522 lysis, and neutralized after a 30-min incubation with 4 µL 15% (wt/vol) NH_4NCO_3.
523 Cellular debris was pelleted, and the supernatant was removed for desiccation by
524 a Savant SpeedVac Concentrator (Thermo Scientific). Desiccated samples were
525 suspended in 100 µL ultra-pure water, and insoluble material was pelleted. The

soluble supernatant was filtered through a Titan syringe filter (PVDF, 0.45 µm, 4 mm) before quantification of c-di-GMP and pGpG using LC-MS/MS on a Quattro Premier XE mass spectrometer (Waters) coupled with an Acquity Ultra Performance LC system (Waters). Cyclic-di-GMP was detected in 10-µL injections of filtered extracts. For the detection of pGpG, filtered extracts were diluted 1:100 in ultra-pure water, and 10-µL injections of the diluted extracts were then analyzed. The intracellular concentrations of c-di-GMP and pGpG were determined by calculating the total number of colony-forming units in each sample and multiplying this value by the intracellular volume of a single bacterium. The total c-di-GMP and pGpG extracted in each sample were then divided by the total intracellular volume of the cells in the sample to provide the intracellular concentration of each analyte.

Metabolite extraction and quantification of c-di-GMP and pGpG in B. subtilis

Three independent replicates of *B. subtilis* 168 WT and Δ*nrnA* Δ*nrnB* were grown overnight in liquid MSgg medium (40) shaking at 37˚C. The following day cultures of each strain were inoculated 1:50 and grown shaking at 37˚C until reaching an optical density at 600 nm (OD_{600}) of 1.0. Metabolite extraction was described previously (45). 5 mL cultures were passed through 0.2 µm nylon filters (EMD Millipore). Metabolism was quenched and metabolites were extracted by inverting the filters into petri dishes that contained 1.5 mL pre-chilled extraction solvent composed of 40:40:20 acetonitrile/methanol/water. Dishes were placed on dry ice for 15 minutes before the wash was collected in

549 microcentrifuge tubes and allowed to spin at max speed for 5 minutes at 4˚C.
550 The supernatant was then transferred to new microcentrifuge tubes and placed in
551 a vacuum centrifuge until metabolite extracts were dry. Detection of c-di-GMP by
552 LC-MS/MS was described previously (46). Briefly, bacterial extract was
553 resuspended in Solvent A (10 mM tributylamine in water, pH 5.0) and centrifuged
554 twice to remove insoluble particles. Metabolites were then separated on a
555 Synergi Fusion-RP column (4 µm particle size, 80 Å pore size, 150 mm x 2 mm,
556 Phenomenex) using a Shimadzu high performance liquid chromatography
557 machine and simultaneously analyzed by a triple quadrupole mass spectrometer
558 (3200 QTRAP, ABSCIEX). The total run time was 20 min at a binary flow rate of
559 0.5 ml min^{-1}, with 10 mM tributylamine in water (pH 5.0) as Solvent A and 100%
560 methanol as Solvent B. The following gradient was performed: 0.01 min, 0% B, 4
561 min, 0% B, 11 min, 50% B, 13 min, 100% B, 15 min, 100% B, 16 min, 0% B, 20
562 min, 0% B. C-di-GMP and pGpG were detected by multiple reaction monitoring
563 (MRM) under negative mode using the ion pairs 689/79 and 689/344 (c-di-GMP)
564 and 707/79 and 707/150 (pGpG). C-di-GMP and pGpG were quantified using the
565 Analyst® software (version 1.6.2) by calculating the total peak area and
566 normalized by total ion current (TIC). Authentic c-di-GMP and pGpG standards
567 were injected and analyzed alongside samples.
568

569 **Figure legends**

570 **Figure 1. A subset of genes with RNase domains reduce aggregation by**
571 **PA14 Δ*orn*.** Photograph of overnight cultures of PA14 Δ*orn* with empty vector
572 (EV), complementation vectors expressing the indicated genes. Genes are
573 grouped by RNase domain. Strains were growing with shaking and induction
574 overnight, allowed to sediment for 30 minutes by gravity, and photographed.
575 Daggers indicate strains grown and induced at 30˚C while the remaining were
576 grown and induced at 37°C. Red boxs indicate genes that prevented
577 autoaggregation.

578

579 **Figure 2. *nrnA*, *nrnB,* and *nrnC* can reduce biofilm formation and**
580 **aggregation by PA14 Δ*orn*.**
581 (A) Quantification of the crystal violet assay for pellicle biofilm formation of the
582 PA14 Δ*orn* strain with either empty vector or complementation by indicated
583 genes carried on a pMMB-based a single-copy IPTG inducible plasmid after 24 h
584 of static growth. (B) Photographs of the aggregation assay and (C) quantification
585 of the crystal violet assay for pellicle biofilm formation of PA14 Δ*orn*
586 complemented with the indicated genes carried on a pMMB-based plasmid.
587 Values shown are the average and SD of three independent experiments. *
588 indicates $p < 0.05$ Students' unpaired two-tailed *t*-test.

589

590 **Figure 3. A subset of RNases can rescue PA14 Δ*orn* pGpG hydrolysis**
591 **defect.** The rate of pGpG cleavage by whole cell lysates of *P. aeruginosa* PA14

592 Δ*orn* complemented with the indicated genes carried on a pMMB-based plasmid.
593 (A) The 3´ to 5´ exoribonucleases from *B. anthracis*, (B) the 3´ to 5´
594 exoribonucleases from *V. cholerae*, and (C) $nrnA_{Bs}$, $nrnB_{Bs}$, $rnjA_{Bs}$,$yhaM_{Bs}$ and
595 $nrnC_{Cc}$. * indicates p < 0.05 Students' unpaired two-tailed *t*-test.
596
597 **Figure 4. Hydrolysis of pGpG by purified RNases.** The rate of ^{32}P-pGpG
598 hydrolysis by 10 nM purified Orn_{Vc}, $NrnA_{Bs}$, $NrnB_{Bs}$, and $NrnC_{Cc}$ incubated with 1
599 μM pGpG supplemented with ^{32}P-pGpG tracer over a period of 30 min. Aliquots
600 were removed for analysis and the reaction was stopped by addition of EDTA at
601 the indicated time points. Radiolabeled nucleotides were separated by TLC and
602 the fraction of ^{32}P-pGpG remaining over total radiolabel was quantified. Values
603 shown are the average and SD of three independent experiments. * indicates p <
604 0.05 Students' unpaired two-tailed *t*-test.
605
606 **Figure 5. Proteins containing HD-GYP domain do not cleave pGpG in cells**
607 **lacking *orn*.** Lysates from PA14 Δ*orn* expressing individual genes encoding an
608 HD-GYP domain from *V. cholerae* were tested for pGpG hydrolysis by monitoring
609 conversion of ^{32}P-pGpG to GMP. Values shown are the average and SD of three
610 independent experiments. * indicates p < 0.05 Students' unpaired two-tailed *t*-
611 test.
612
613 **Figure 6. Cyclic di-GMP fluorescence riboswitch detection of c-di-GMP**
614 **levels in *B. subtilis* 168.** Representative images of fluorescence of the

615 constitutively expressed YFP reporter P_{const}-*yfp* (A) or the c-di-GMP riboswitch
616 reporter construct P_{const}-*lchAA* UTR-*yfp* (B) in either *B. subtilis* 168 wild type (WT)
617 or the double deletion mutant Δ*nrnA* Δ*nrnB*. Histograms of the quantification of
618 average fluorescence intensity of *B. subtilis* 168 wild type and Δ*nrnA* Δ*nrnB* with
619 P_{const}-*yfp* (C) or P_{const}-*lchAA* UTR-*yfp* cells (D) (n ~ 300).
620
621 **Figure 7. Model for degradation of cyclic dinucleotides.** Cartoon of the two-
622 step degradation process of (A) c-di-GMP, (B) c-di-AMP, and (C) cGAMP. Step 1
623 is cyclic dinucleotides linearization (indicated by the gray boxes). Step 2 is pNpN
624 hydrolysis (indicated by the green boxes). In scenarios in which the linear
625 dinucleotide accumulates, there is feedback inhibition on the enzymes that
626 linearize cyclic dinucleotides. Dashed lines indicate potential inhibition and ?
627 mark indicate the presence of additional categories of enzymes that hydrolyze
628 dinucleotides.
629
630 **Table 1. Intracellular concentration of pGpG following complementation of**
631 **PA14 Δ*orn* strains**

Strain	μM pGpG*	μM c-di-GMP*
Wild type pMMB	2.2 ± 0.4	0.016 ± 0.008
Δ*orn* pMMB	17.4 ± 3.7	0.58 ± 0.10
Δ*orn* pMMB-orn_{Pa}	5.2 ± 1.4	0.028 ± 0.013
Δ*orn* pMMB-orn_{Vc}	6.5 ± 1.8	0.017 ± 0.011
Δ*orn* pMMB-$nrnA_{Bs}$	3.6 ± 1.4	0.022 ± 0.016

Δ*orn* pMMB-*nrnA*$_{Bs}$	3.3 ± 1.2	0.024 ± 0.012
Δ*orn* pMMB-*nrnB*$_{Bs}$	2.5 ± 1.1	0.023 ± 0.011
Δ*orn* pMMB-*nrnC*$_{Cc}$	2.4 ± 1.1	0.020 ± 0.001

[*] average and standard deviation of 3 experiments, calculated assuming the volume of a single bacterium equals 4.3×10^{-1} fL (9).

Table 2. Intracellular concentration of pGpG and c-di-GMP in *B. subtilis* and Δ*nrnA* Δ*nrnB* strains

		WT 168 (□M)	Δ*nrnA* Δ*nrnB* (□M)	Fold Change (Δ/WT)
pGpG	daughter ion 1	ND	1.8 ± 0.6	NA
	daughter ion 2	ND	1.8 ± 0.4	NA
c-di-GMP	daughter ion 1	0.8 ± 0.2	2.4 ± 0.5	3.0
	daughter ion 2	0.9 ± 0.1	3.0 ± 0.9	3.3

Journal of Bacteriology

JB

Journal of Bacteriology

640 **Acknowledgments**

641

642 We would like to acknowledge our funding from National Institute of Allergy and
643 Infectious Diseases (NIAID) R01-AI110740 to V.T. L., Cystic Fibrosis Foundation
644 (CF Foundation) LEE16G0 to V.T. L., National Institutes of Health R01-
645 GM109259 to C.M.W., and National Science Foundation (NSF) MCB1051440 to
646 W.C.W. C.A.W. was supported in part by the National Institutes of Health (NIH)
647 training grant T32-GM080201.

References

1. **Ross P, Weinhouse H, Aloni Y, Michaeli D, Ohana P, Mayer R, Braun S, de Vroom GE, van der Marel A, van Boom JH, Benziman M.** 1987. Regulation of cellulose synthesis in *Acetobacter xylinum* by cyclic diguanylic acid. Nature **325:**279-281.
2. **Römling U, Galperin MY, Gomelsky M.** 2013. Cyclic di-GMP: the first 25 years of a universal bacterial second messenger. Microbiol Mol Biol Rev **77:**1-52.
3. **Ausmees N, Mayer R, Weinhouse H, Volman G, Amikam D, Benziman M, Lindberg M.** 2001. Genetic data indicate that proteins containing the GGDEF domain possess diguanylate cyclase activity. FEMS Microbiol Lett **204:**163-167.
4. **Simm R, Morr M, Kader A, Nimtz M, Römling U.** 2004. GGDEF and EAL domains inversely regulate cyclic di-GMP levels and transition from sessility to motility. Mol Microbiol **53:**1123-1134.
5. **Ryjenkov DA, Tarutina M, Moskvin OV, Gomelsky M.** 2005. Cyclic diguanylate is a ubiquitous signaling molecule in bacteria: insights into biochemistry of the GGDEF protein domain. J Bacteriol **187:**1792-1798.
6. **Tamayo R, Tischler AD, Camilli A.** 2005. The EAL domain protein VieA is a cyclic diguanylate phosphodiesterase. J Biol Chem **280:**33324-33330.
7. **Schmidt AJ, Ryjenkov DA, Gomelsky M.** 2005. The ubiquitous protein domain EAL is a cyclic diguanylate-specific phosphodiesterase: enzymatically active and inactive EAL domains. J Bacteriol **187:**4774-4781.
8. **Galperin MY, Nikolskaya AN, Koonin EV.** 2001. Novel domains of the prokaryotic two-component signal transduction systems. FEMS Microbiol Lett **203:**11-21.
9. **Orr MW, Donaldson GP, Severin GB, Wang J, Sintim HO, Waters CM, Lee VT.** 2015. Oligoribonuclease is the primary degradative enzyme for pGpG in *Pseudomonas aeruginosa* that is required for cyclic-di-GMP turnover. Proc Natl Acad Sci U S A **112:**E5048-5057.
10. **Cohen D, Mechold U, Nevenzal H, Yarmiyhu Y, Randall TE, Bay DC, Rich JD, Parsek MR, Kaever V, Harrison JJ, Banin E.** 2015. Oligoribonuclease is a central feature of cyclic diguanylate signaling in *Pseudomonas aeruginosa*. Proc Natl Acad Sci U S A **112:**11359-11364.
11. **Niyogi SK, Datta AK.** 1975. A novel oligoribonuclease of *Escherichia coli*. I. Isolation and properties. J Biol Chem **250:**7307-7312.
12. **Datta AK, Niyogi K.** 1975. A novel oligoribonuclease of *Escherichia coli*. II. Mechanism of action. J Biol Chem **250:**7313-7319.
13. **Ghosh S, Deutscher MP.** 1999. Oligoribonuclease is an essential component of the mRNA decay pathway. Proc Natl Acad Sci U S A **96:**4372-4377.
14. **Mechold U, Fang G, Ngo S, Ogryzko V, Danchin A.** 2007. YtqI from *Bacillus subtilis* has both oligoribonuclease and pAp-phosphatase activity. Nucleic Acids Res **35:**4552-4561.

15. **Fang M, Zeisberg WM, Condon C, Ogryzko V, Danchin A, Mechold U.** 2009. Degradation of nanoRNA is performed by multiple redundant RNases in *Bacillus subtilis*. Nucleic Acids Res **37:**5114-5125.
16. **Liu MF, Cescau S, Mechold U, Wang J, Cohen D, Danchin A, Boulouis HJ, Biville F.** 2012. Identification of a novel nanoRNase in *Bartonella*. Microbiology **158:**886-895.
17. **Oussenko IA, Sanchez R, Bechhofer DH.** 2002. *Bacillus subtilis* YhaM, a member of a new family of 3'-to-5' exonucleases in gram-positive bacteria. J Bacteriol **184:**6250-6259.
18. **Mathy N, Benard L, Pellegrini O, Daou R, Wen T, Condon C.** 2007. 5'-to-3' exoribonuclease activity in bacteria: role of RNase J1 in rRNA maturation and 5' stability of mRNA. Cell **129:**681-692.
19. **Kulasakara H, Lee V, Brencic A, Liberati N, Urbach J, Miyata S, Lee DG, Neely AN, Hyodo M, Hayakawa Y, Ausubel FM, Lory S.** 2006. Analysis of *Pseudomonas aeruginosa* diguanylate cyclases and phosphodiesterases reveals a role for bis-(3'-5')-cyclic-GMP in virulence. Proc Natl Acad Sci U S A **103:**2839-2844.
20. **Lee VT, Matewish JM, Kessler JL, Hyodo M, Hayakawa Y, Lory S.** 2007. A cyclic-di-GMP receptor required for bacterial exopolysaccharide production. Mol Microbiol **65:**1474-1484.
21. **Andrade JM, Pobre V, Silva IJ, Domingues S, Arraiano CM.** 2009. The role of 3'-5' exoribonucleases in RNA degradation. Prog Mol Biol Transl Sci **85:**187-229.
22. **Condon C.** 2003. RNA processing and degradation in *Bacillus subtilis*. Microbiol Mol Biol Rev **67:**157-174, table of contents.
23. **Bechhofer DH.** 2011. *Bacillus subtilis* mRNA decay: new parts in the toolkit. Wiley Interdiscip Rev RNA **2:**387-394.
24. **Condon C.** 2010. What is the role of RNase J in mRNA turnover? RNA Biol **7:**316-321.
25. **Eddy SR.** 2011. Accelerated Profile HMM Searches. PLoS Comput Biol **7:**e1002195.
26. **Finn RD, Clements J, Eddy SR.** 2011. HMMER web server: interactive sequence similarity searching. Nucleic Acids Res **39:**W29-37.
27. **Rolfs A, Montor WR, Yoon SS, Hu Y, Bhullar B, Kelley F, McCarron S, Jepson DA, Shen B, Taycher E, Mohr SE, Zuo D, Williamson J, Mekalanos J, Labaer J.** 2008. Production and sequence validation of a complete full length ORF collection for the pathogenic bacterium *Vibrio cholerae*. Proc Natl Acad Sci U S A **105:**4364-4369.
28. **O'Toole GA, Kolter R.** 1998. Initiation of biofilm formation in *Pseudomonas fluorescens* WCS365 proceeds via multiple, convergent signalling pathways: a genetic analysis. Mol Microbiol **28:**449-461.
29. **Huynh TN, Luo S, Pensinger D, Sauer JD, Tong L, Woodward JJ.** 2015. An HD-domain phosphodiesterase mediates cooperative hydrolysis of c-di-AMP to affect bacterial growth and virulence. Proc Natl Acad Sci U S A **112:**E747-756.

30. **Rao F, See RY, Zhang D, Toh DC, Ji Q, Liang ZX.** 2010. YybT is a signaling protein that contains a cyclic dinucleotide phosphodiesterase domain and a GGDEF domain with ATPase activity. J Biol Chem **285:**473-482.
31. **Bowman L, Zeden MS, Schuster CF, Kaever V, Grundling A.** 2016. New Insights into the Cyclic di-adenosine Monophosphate (c-di-AMP) Degradation Pathway and the Requirement of the Cyclic Dinucleotide for Acid Stress Resistance in *Staphylococcus aureus*. J Biol Chem **291:**26970-26986.
32. **Davies BW, Bogard RW, Young TS, Mekalanos JJ.** 2012. Coordinated regulation of accessory genetic elements produces cyclic di-nucleotides for *V. cholerae* virulence. Cell **149:**358-370.
33. **Gao J, Tao J, Liang W, Zhao M, Du X, Cui S, Duan H, Kan B, Su X, Jiang Z.** 2015. Identification and characterization of phosphodiesterases that specifically degrade 3'3'-cyclic GMP-AMP. Cell Res **25:**539-550.
34. **Hammer BK, Bassler BL.** 2009. Distinct sensory pathways in *Vibrio cholerae* El Tor and classical biotypes modulate cyclic dimeric GMP levels to control biofilm formation. J Bacteriol **191:**169-177.
35. **McKee RW, Kariisa A, Mudrak B, Whitaker C, Tamayo R.** 2014. A systematic analysis of the in vitro and in vivo functions of the HD-GYP domain proteins of *Vibrio cholerae*. BMC Microbiol **14:**272.
36. **Koo BM, Kritikos G, Farelli JD, Todor H, Tong K, Kimsey H, Wapinski I, Galardini M, Cabal A, Peters JM, Hachmann AB, Rudner DZ, Allen KN, Typas A, Gross CA.** 2017. Construction and Analysis of Two Genome-Scale Deletion Libraries for *Bacillus subtilis*. Cell Syst **4:**291-305 e297.
37. **Jarmer H, Berka R, Knudsen S, Saxild HH.** 2002. Transcriptome analysis documents induced competence of *Bacillus subtilis* during nitrogen limiting conditions. FEMS Microbiol Lett **206:**197-200.
38. **Roelofs KG, Wang J, Sintim HO, Lee VT.** 2011. Differential radial capillary action of ligand assay for high-throughput detection of protein-metabolite interactions. Proc Natl Acad Sci U S A **108:**15528-15533.
39. **Donaldson GP, Roelofs KG, Luo Y, Sintim HO, Lee VT.** 2012. A rapid assay for affinity and kinetics of molecular interactions with nucleic acids. Nucleic Acids Res **40:**e48.
40. **Branda SS, Chu F, Kearns DB, Losick R, Kolter R.** 2006. A major protein component of the *Bacillus subtilis* biofilm matrix. Mol Microbiol **59:**1229-1238.
41. **Paintdakhi A, Parry B, Campos M, Irnov I, Elf J, Surovtsev I, Jacobs-Wagner C.** 2016. Oufti: an integrated software package for high-accuracy, high-throughput quantitative microscopy analysis. Mol Microbiol **99:**767-777.
42. **Schindelin J, Arganda-Carreras I, Frise E, Kaynig V, Longair M, Pietzsch T, Preibisch S, Rueden C, Saalfeld S, Schmid B, Tinevez JY, White DJ, Hartenstein V, Eliceiri K, Tomancak P, Cardona A.** 2012. Fiji: an open-source platform for biological-image analysis. Nat Methods **9:**676-682.
43. **Massie JP, Reynolds EL, Koestler BJ, Cong JP, Agostoni M, Waters CM.** 2012. Quantification of high-specificity cyclic diguanylate signaling. Proc Natl Acad Sci U S A **109:**12746-12751.

44. **Severin GB, Waters CM.** 2017. Spectrophotometric and Mass Spectroscopic Methods for the Quantification and Kinetic Evaluation of In Vitro c-di-GMP Synthesis. Methods Mol Biol **1657:**71-84.
45. **Liu K, Myers AR, Pisithkul T, Claas KR, Satyshur KA, Amador-Noguez D, Keck JL, Wang JD.** 2015. Molecular mechanism and evolution of guanylate kinase regulation by (p)ppGpp. Mol Cell **57:**735-749.
46. **Tu BP, Mohler RE, Liu JC, Dombek KM, Young ET, Synovec RE, McKnight SL.** 2007. Cyclic changes in metabolic state during the life of a yeast cell. Proc Natl Acad Sci U S A **104:**16886-16891.

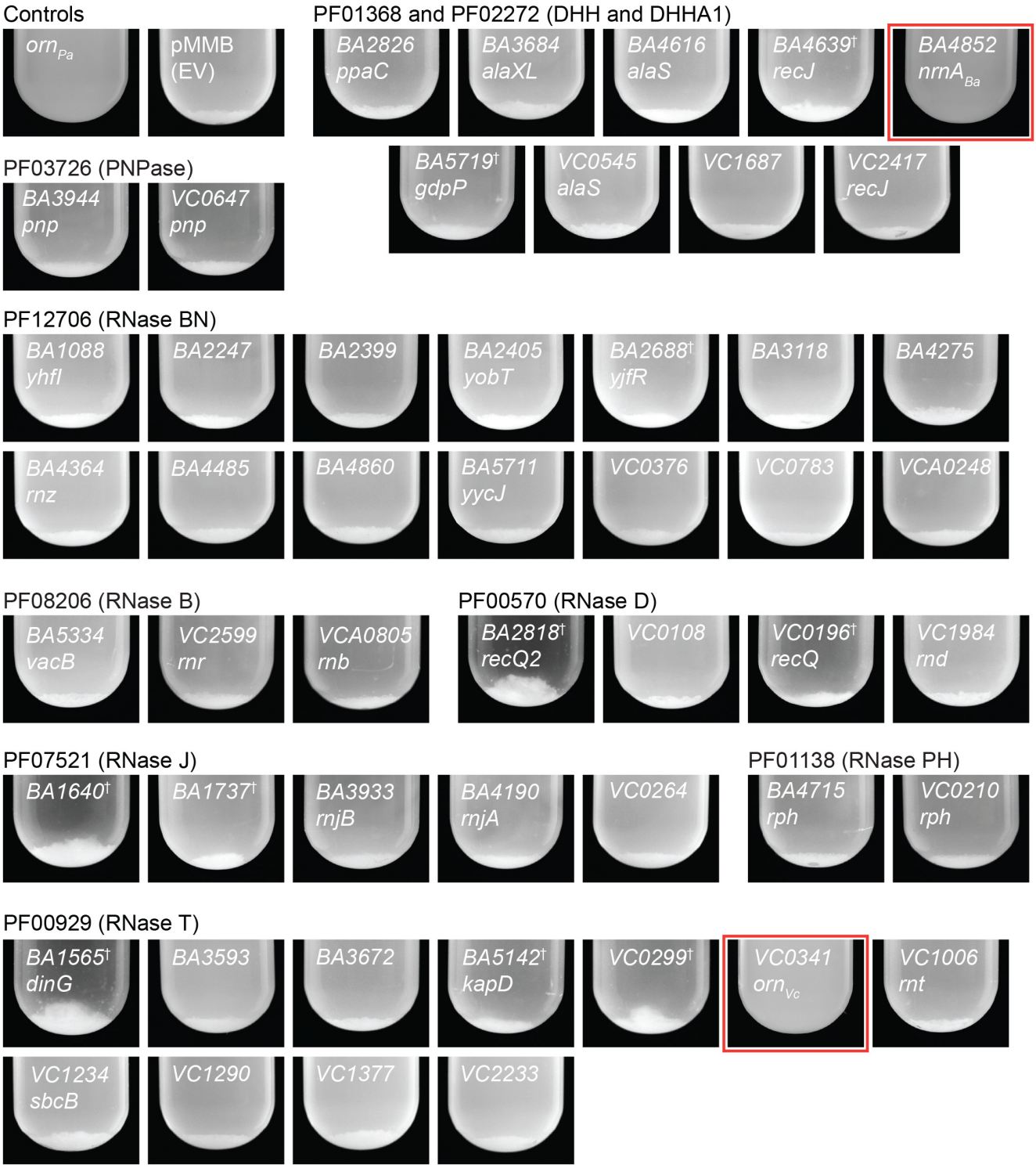

Figure 1. A subset of genes with RNase domains reduce aggregation by PA14 Δ*orn*.

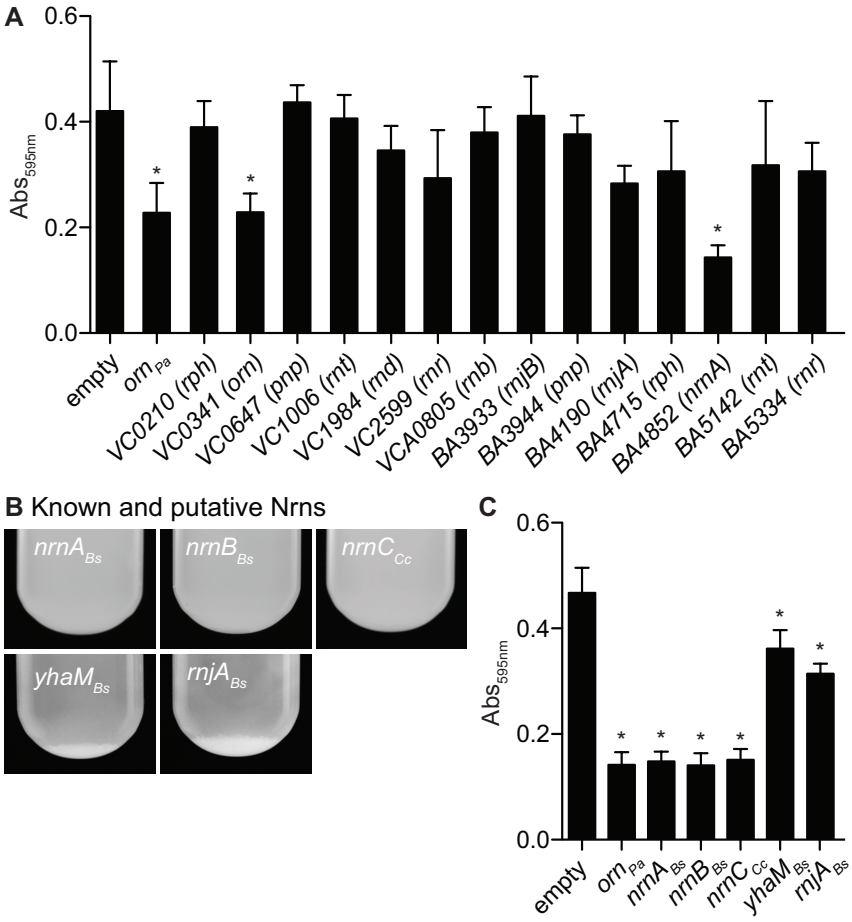

Figure 2. *nrnA*, *nrnB* and *nrnC* can reduce biofilm formation and aggregation by PA14 Δ*orn*.

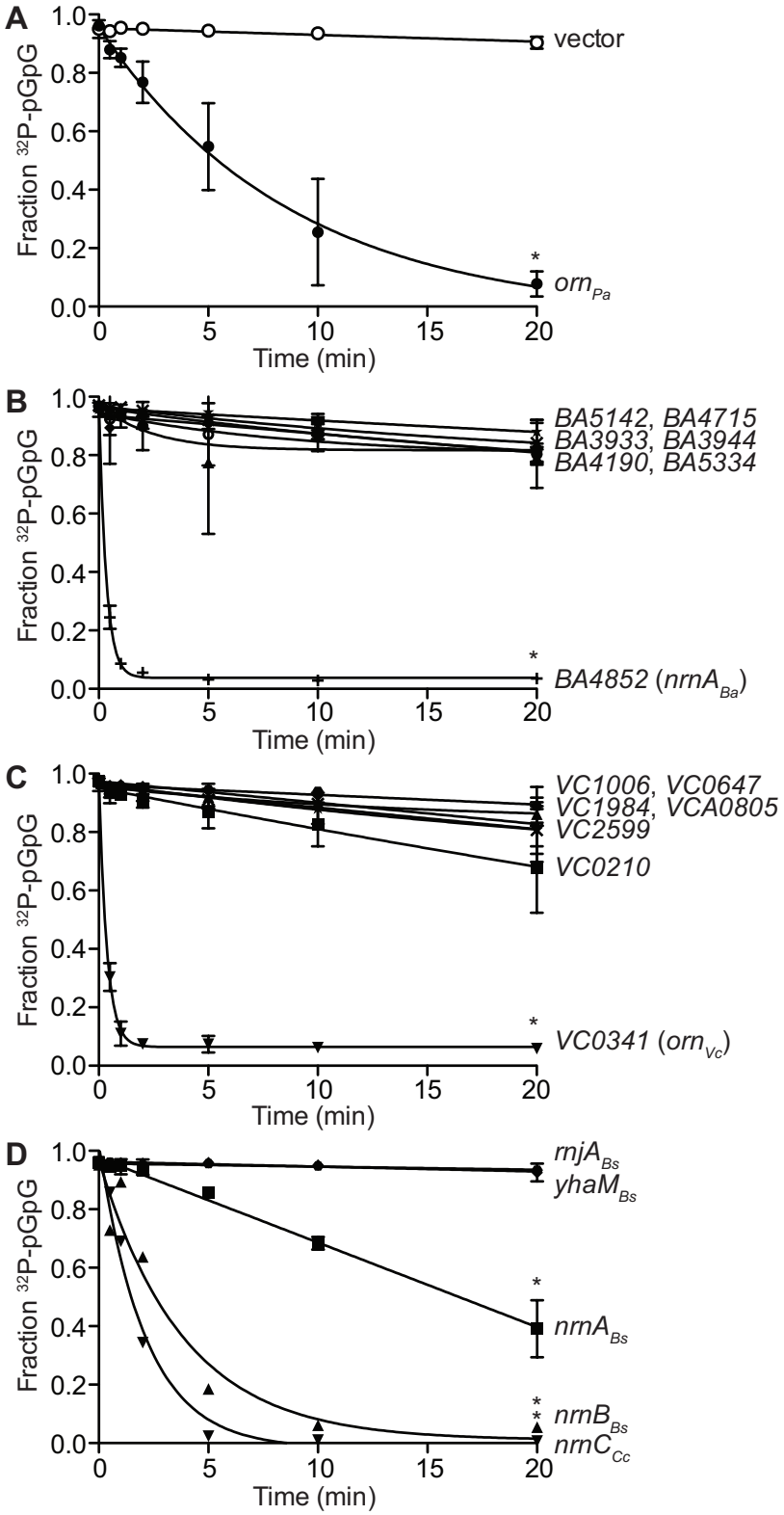

Figure 3. A subset of RNases can rescue PA14 Δ*orn* pGpG hydrolysis defect.

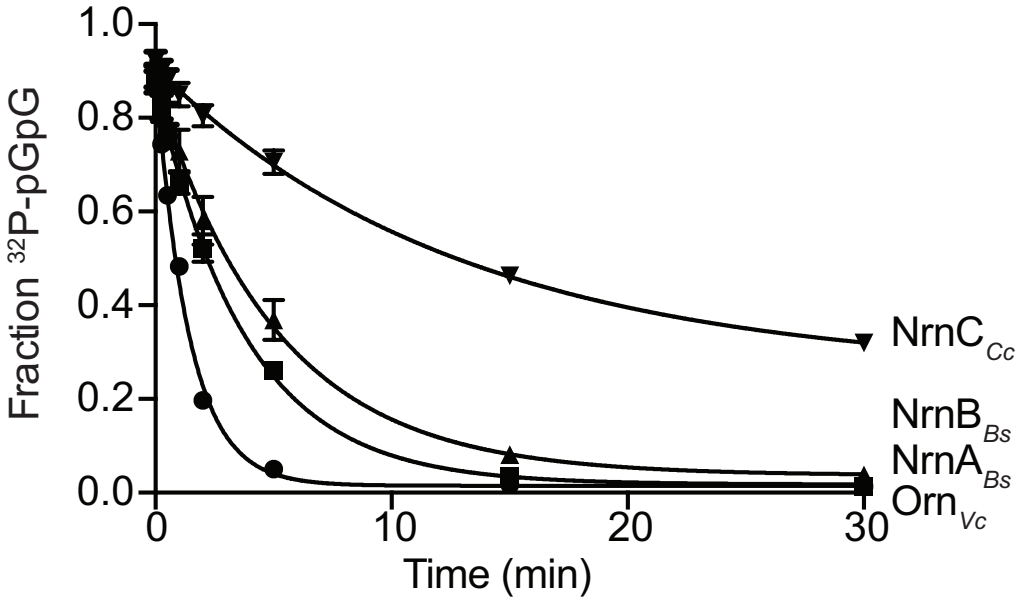

Figure 4. Hydrolysis of pGpG by purified RNases.

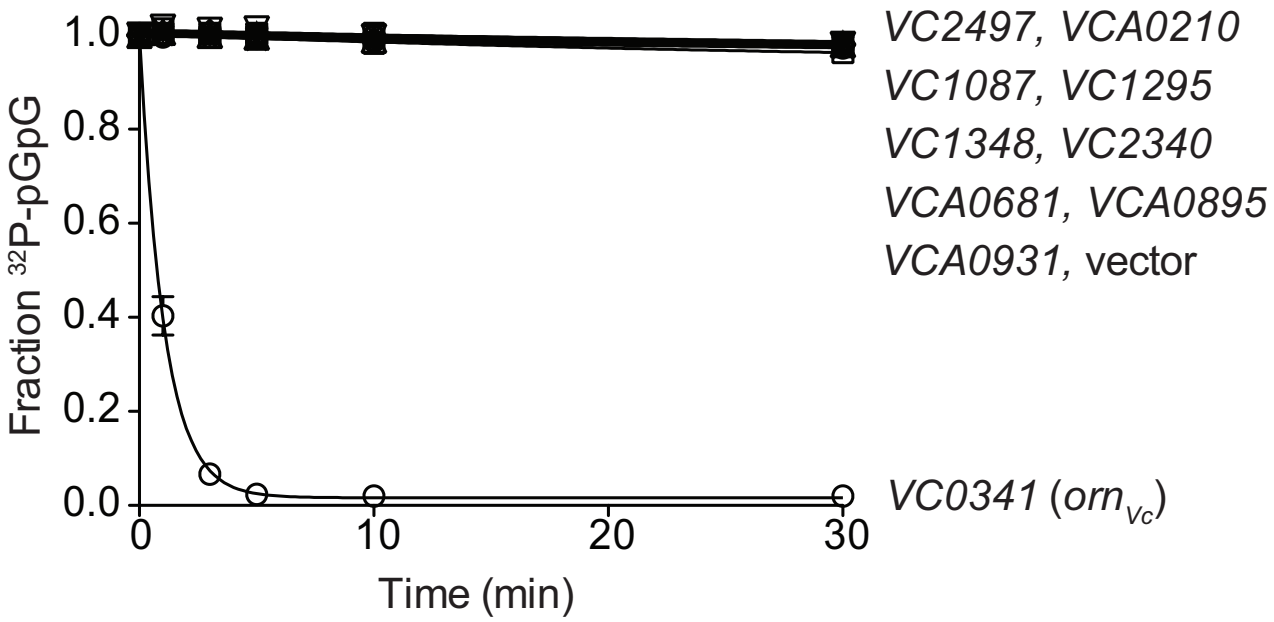

Figure 5. Proteins containing HD-GYP domain do not cleave pGpG in cells lacking *orn*.

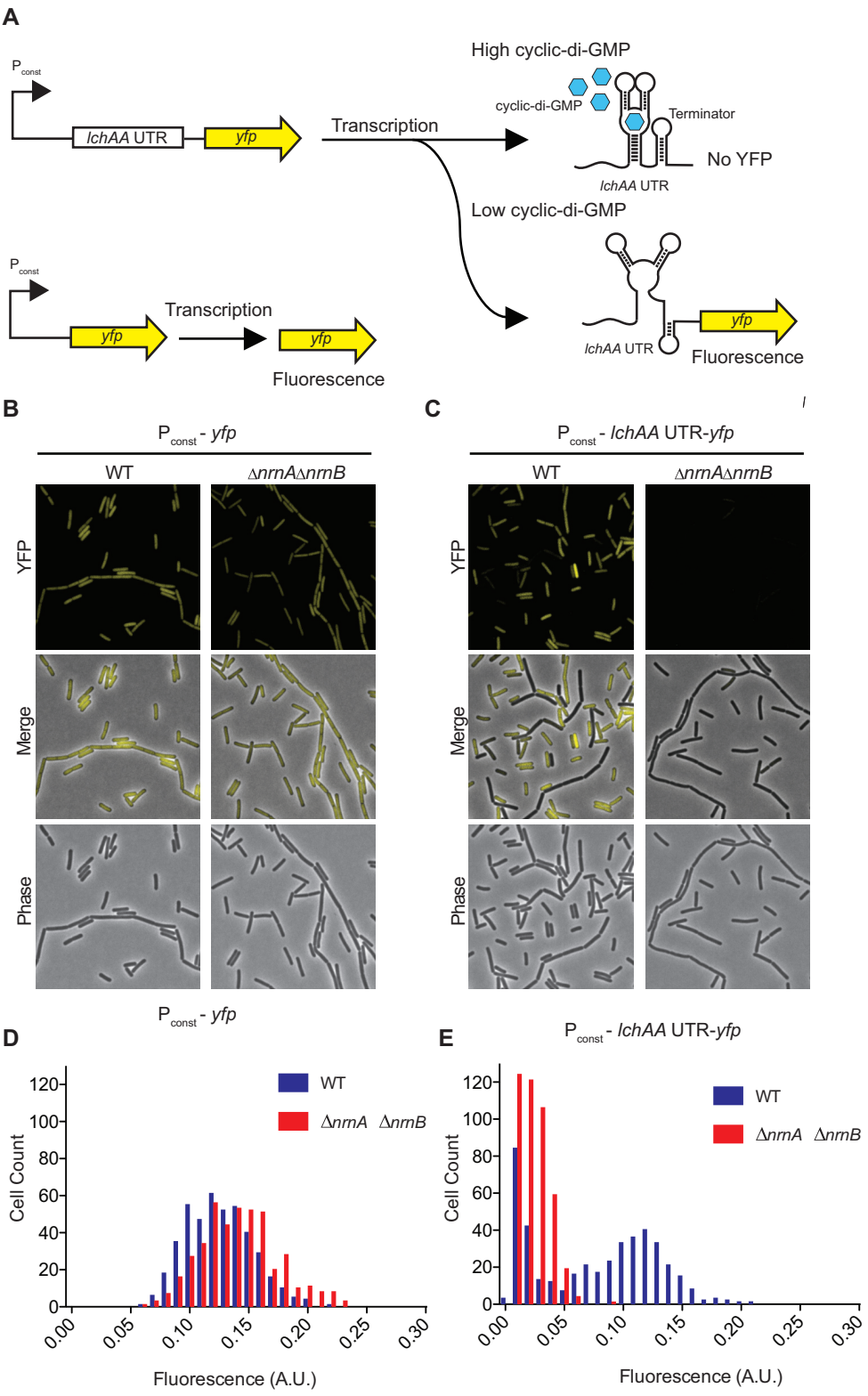

Figure 6. Cyclic di-GMP fluorescence riboswitch detection of c-di-GMP levels in *B. subtilis* 168.

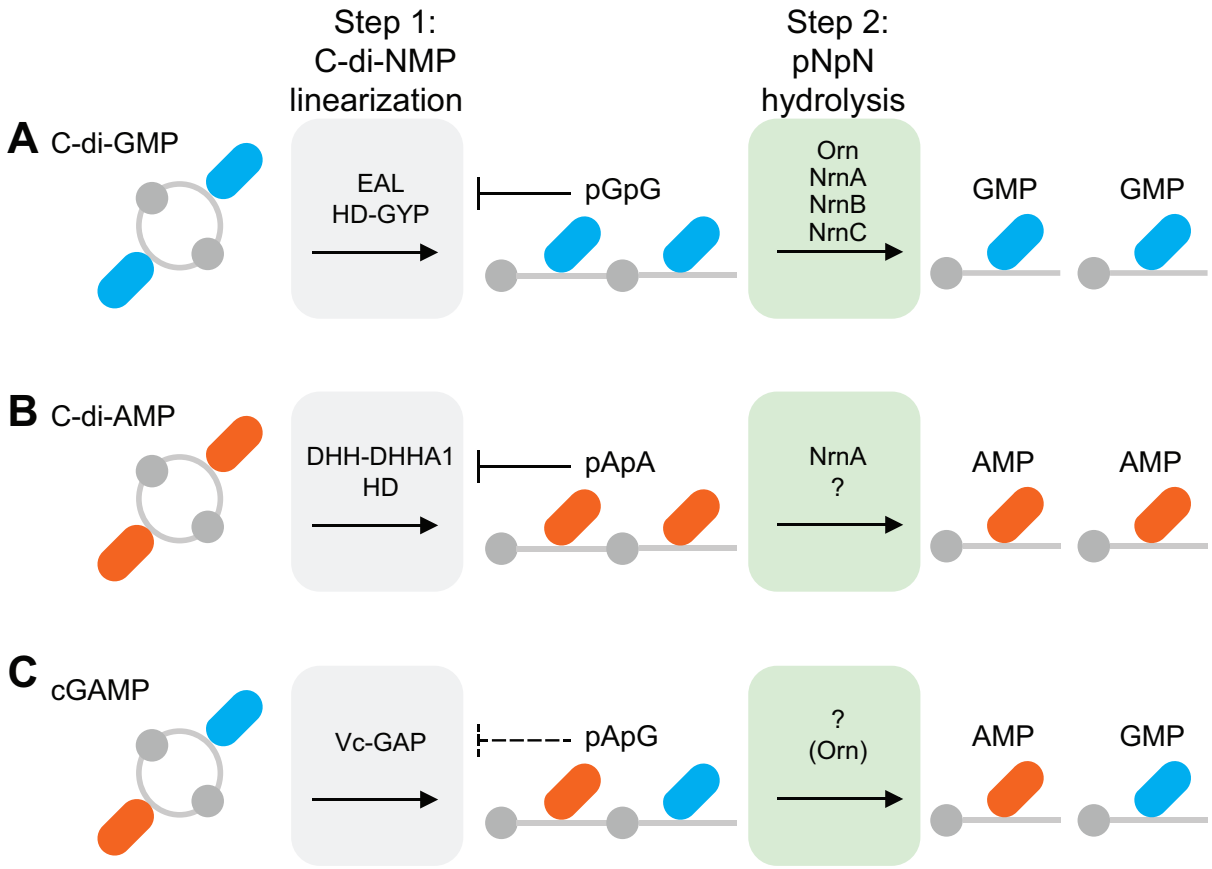

Figure 7. Model for degradation of cyclic dinucleotides.